NANO LETTERS

pubs.acs.org/NanoLett

Three-Dimensional Carbon Nanotube–Textile Anode for High-Performance Microbial Fuel Cells

Xing Xie,[†] Liangbing Hu,[‡] Mauro Pasta,[‡,§] George F. Wells,[†] Desheng Kong,[‡] Craig S. Criddle,*[,†] and Yi Cui*[,‡]

Department of Civil and Environmental Engineering and Department of Material Science and Engineering, Stanford University, Stanford, California 94305, United States, and Dipartimento di Chimica Inorganica, Metallorganica e Analitica "Lamberto Malatesta", Università degli Studi di Milano, Via Venezian 21, 20133 Milano, Italy

ABSTRACT Microbial fuel cells (MFCs) harness the metabolism of microorganisms, converting chemical energy into electrical energy. Anode performance is an important factor limiting the power density of MFCs for practical application. Improving the anode design is thus important for enhancing the MFC performance, but only a little development has been reported. Here, we describe a biocompatible, highly conductive, two-scale porous anode fabricated from a carbon nanotube–textile (CNT–textile) composite for high-performance MFCs. The macroscale porous structure of the intertwined CNT–textile fibers creates an open 3D space for efficient substrate transport and internal colonization by a diverse microflora, resulting in a 10-fold-larger anolyte–biofilm–anode interfacial area than the projective surface area of the CNT–textile. The conformally coated microscale porous CNT layer displays strong interaction with the microbial biofilm, facilitating electron transfer from exoelectrogens to the CNT–textile anode. An MFC equipped with a CNT–textile anode has a 10-fold-lower charge-transfer resistance and achieves considerably better performance than one equipped with a traditional carbon cloth anode: the maximum current density is 157% higher, the maximum power density is 68% higher, and the energy recovery is 141% greater.

KEYWORDS Three-dimensional electrode, microbial fuel cells, two-scale porous structure, anolyte–biofilm–anode interface, extracellular electron transfer, textile

Microbial fuel cells (MFCs) convert chemical energy into electrical energy by the catalytic activity of microorganisms.[1−5] Promising applications include energy recovery from wastewater,[6] marine sediment,[7] and human excrement in space.[8] The basic operation of MFCs is similar to that of other fuel cells (Figure S1): the oxidation of an electron donor at an anode releases electrons that pass through an external circuit to a cathode where an oxidant, such as oxygen, is reduced. In MFCs, however, oxidation at the anode is mediated by "exoelectrogens", microorganisms that transfer electrons to an electrode.[1] The transfer of electrons may occur by direct contact between redox-active membrane-bound proteins and the electrode surface, by the diffusion of redox-active molecules that ferry electrons between the electrode surface and the cell, or by conduction through microbially generated nanowires (or a solid matrix) that link cells to the electrode surface (Figure 1A).[1,3,9] Besides high conductivity, chemical stability, biocompatibility, resistance to decomposition, and catalytic activity, optimal anodes preferably require porous structure to allow internal colonization and strong interaction, including affinitive mechanical contact and higher electrical conductivity, between an anode surface and microbial biofilms to faciliate extracellular electron transfer.

Researchers have employed various commercially available carbon-based porous anodes in MFCs, including carbon cloth,[10] carbon paper,[11] carbon foam,[5] and reticulated vitrified carbon.[12] However, rapid microbial growth can clog the pores in these materials easily and hence hinder the diffusion of the substate, making the inner anode surface unfavorable for microbial colonization.[4] New developments on anode structure or materials have recently been reported. Logan and colleagues recently detailed the invention of a graphite fiber brush anode that provides a large specific surface area of 7170–18 200 m^2 m^{-3}, depending on the anode size.[13] However, the space between the fibers is not uniformly distributed within the brush, and evidence that the entire graphite fiber surface is accessible to microorganisms remains to be collected. To improve the interaction between the anode surface and microbial biofilm, several studies have investigated carbon-based anodes modified with polymers[14,15] or carbon nanotubes (CNTs).[16] Moreover, several new composite anodes have also been reported.[17−19] However, none of these have an open macroscale porous structure to enlarge the anolyte–biofilm–anode interfacial

* To whom correspondence should be addressed. E-mail: ccriddle@stanford.edu or yicui@stanford.edu.

[†] Department of Civil and Environmental Engineering, Stanford University.

[‡] Department of Material Science and Engineering, Stanford University.

[§] Università degli Studi di Milano.

Received for review: 11/6/2010
Published on Web: 00/00/0000

DOI: 10.1021/nl103905t | *Nano Lett.* **XXXX,** *xxx,* 000–000

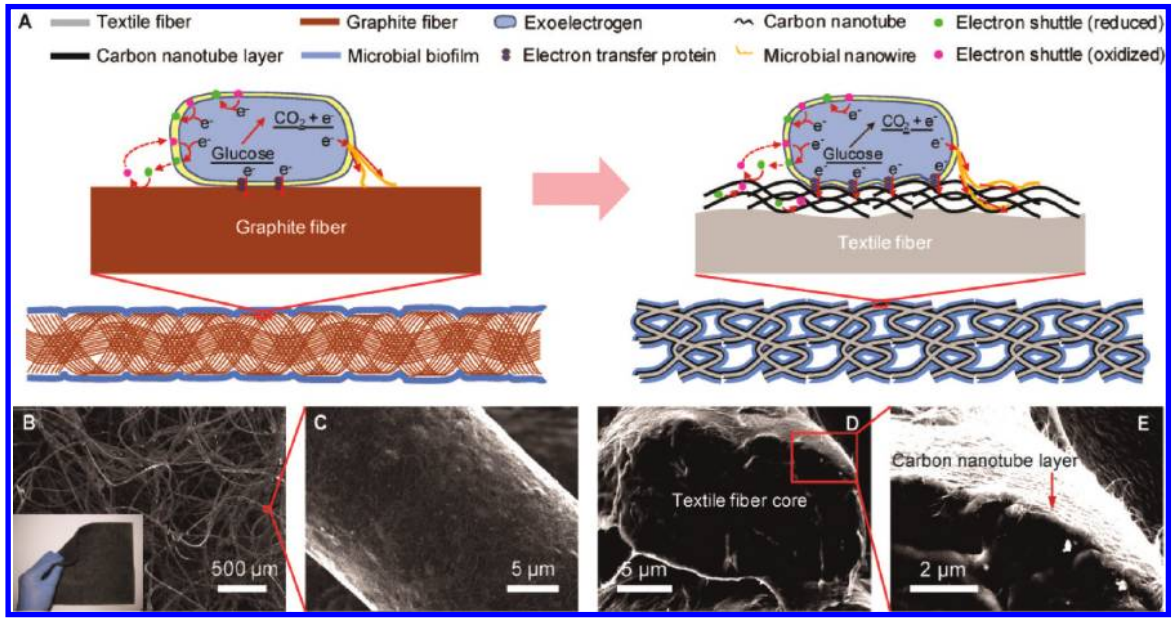

FIGURE 1. Carbon nanotube−textile (CNT−textile) composite. (A) Schematic of the electrode configuration and electron-transfer mechanisms for the CNT−textile anode (right), compared with the widely used carbon cloth anode (left). (B) Scanning electron microscope (SEM) image of the CNT−textile showing the open macroscale porous structure. The inset is a 15 cm ×15 cm piece of CNT−textile with a sheet resistance of 4 Ω square^{-1}. (C) SEM image of a textile fiber conformally coated with CNTs. (D, E) Cross section of a CNT−textile fiber. The diameter of the CNT−textile fiber is about 20 μm, and the thickness of the CNT coating is about 200 nm.

area. To date, anode performance remains one of the most important factors limiting the power density of MFCs for practical application.[20−22]

In this study, we propose a 3D anode configuration design that combines an open macrocale porous structure for internal microbial colonization and an affinitive anode surface for improved electron transfer. The basic anode material requirements of conductivity, stability, and biocompatibility also need to be satisfied. This configuration design was realized by conformally coating CNTs on a macroscale porous textile made of randomly intertwined polyester fibers with diameters of approximately 20 μm.[23] (For synthesis details, see the Materials and Methods section in the Supporting Information.) Herein we refer to this composite as a CNT−textile. Such a CNT−textile anode provides a two-scale porous structure, namely, a microscale porous CNT layer coated onto a macroscale porous textile. We found that the macroscale porous textile provides an open 3D space accessible to microbial growth whereas the microscale porous CNT layer shows strong interactions with the microbial biofilm. Compared with a widely used commercial carbon cloth anode, our CNT−textile achieved significantly improved MFC performance. The CNT−textile is also very conductive, chemically and mechanically stable, and biocompatible. In addition, it is light in weight and easy to prepare, and thus this novel material shows great promise for large-scale practical application.

Figure 1A shows a schematic of the electrode configuration and electron-transfer mechanisms of our CNT−textile anode (right), compared with a widely used carbon cloth anode (left). In the CNT−textile, the intertwined macroscale textile fibers (Figure 1B) create a 3D space (on the order of 100 μm), which is designed to allow the substrate transport and colonization of microorganisms (blue film in Figure 1A, right) deep inside the whole electrode to achieve an exceptionally high anolyte−biofilm−anode interfacial area. This will be a significant advantage over carbon cloth anodes, which do not have suitable macroscale pores, resulting in the formation of a biofilm only on the outside surfaces of the electrodes (Figure 1A, left). CNTs conformally coat the textile fibers, following their original morphology (Figure 1C,D). Even with only an ∼200-nm-thick CNT coating (Figure 1E), the CNT−textile achieves excellent conductance (50 S cm^{-1}, Figure S2) even if calculated using the whole cross-sectional area of the CNT−textile fiber. The conductivity of CNT films only is 1250 S cm^{-1}. This highly conductive CNT network with microscale pores is expected to provide a strong interaction with microbial biofilms (Figure 1A, right; enlarged area in scheme) and facilitate electron transfer. To test the hypothesis that our CNT−textile satisfies the desired 3D anode configuration and improves the extracellular electron-transfer efficiency, the CNT−textile was installed as the anode in a classic H-shaped two-chambered MFC. (For the experimental setup, see Figure S3 and the Materials and Methods section in the Supporting Information.)

The MFC was inoculated with domestic wastewater and fed glucose. The uncolonized CNT−textile was initially inactive (Figure 2A). After 12 days of operation, the operating voltage increased to greater than 0.3 V across a 1 kΩ resistor (Figure 2B), indicating a successful startup.[1] During this period, the anode was colonized, and the anode compartment became turbid (Figure S3). The cyclic voltammogram (Figure 2A) dem-

DOI: 10.1021/nl103905t | *Nano Lett.* **XXXX,** *xxx,* 000−000

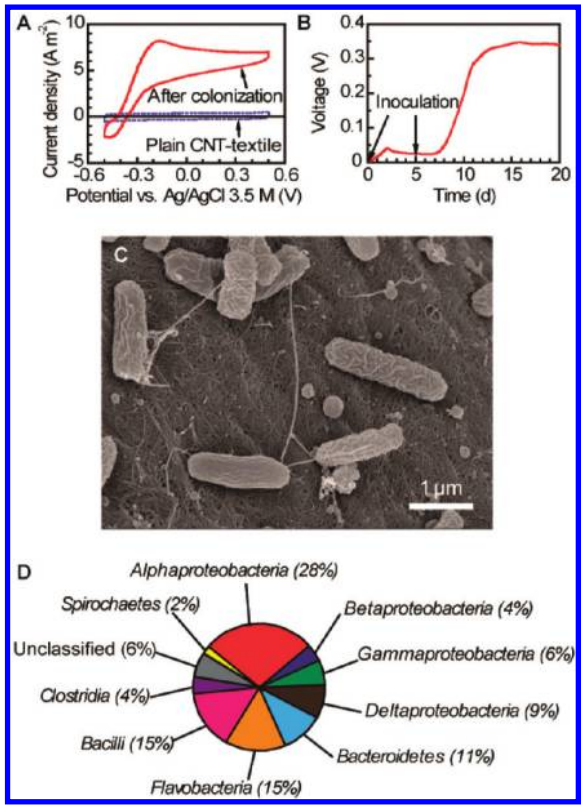

FIGURE 2. Startup of the MFC equipped with a CNT−textile anode. (A) Cyclic voltammograms for the CNT−textile anode before and after colonization. A positive current indicates glucose oxidation. The scan rate was 10 mV s^{-1}. (B) Voltage generation of the MFC across a 1 kΩ external resistor. An operating voltage that is higher than 0.3 V indicates successful startup. (C) SEM image of the microorganisms on the CNT layer. (D) Structure of the microbial community on the CNT−textile anode based on a 16S rRNA gene clone library.

onstrated a significant positive current peak for glucose oxidation, which is evidence of exoelectrogenic activity. A scanning electron microscope (SEM) image (Figure 2C) provided evidence of the colonization and biocompatibility of the CNT−textile anode. CNTs are promising for use as electrodes in fuel cells because of their extraordinarily high conductivity, mechanical flexibility, and large specific surface area.[24−26] A possible concern for MFCs is biocompatibility: CNTs could be inhibitory or even toxic to microorganisms.[27,28] For the CNT−textile anode, although the textile fiber provided mechanical support, the sole electroactive material present was CNT. Therefore, our results confirm that CNT is biocompatible in MFCs and can function as an anode alone. The microbial community structure of the biofilm associated with the CNT−textile anode was analyzed via a bacterial 16S rRNA gene clone library. The results revealed a diverse community (Figure 2D), including taxa previously reported in MFCs and related to *Geobacter*, *Rhodopseudomonas*, *Ochrobactrum*, and *Enterobacter* (Figure S4).[1,3] The observed phylogenetic diversity likely reflects the biochemical/metabolic diversity that occurs when glucose is fermented and its fermentation products are then oxidized.[29,30] Stable operation of this MFC has been achieved for more than 4 months (Figure S5).

The performance of MFCs is affected by many factors, including the cathodic reaction,[31] substrate,[32] buffer system,[33] and operating temperature.[34] Moreover, researchers reported the MFC performance with different parameters obtained by various methods.[35−37] Therefore, it is difficult to compare the MFC performance directly between different studies. To evaluate the performance of the CNT−textile anode, we thus operated an MFC with an identical configuration but with a widely used commercial carbon cloth anode in parallel with our CNT−textile-equipped MFC. The carbon cloth is made of regularly woven graphite fibers (Figure S6). On the basis of the physical parameters provided by the merchant (Fuel Cell Earth LLC, MA) or obtained from direct measurements, the porosities of the CNT−textile anode and the carbon cloth anode were calculated to be 95.8 and 64.6 %, respectively. A greater porosity of the CNT−textile provides more space for substrate transport and colonization. After 55 days of operation, both anodes were sampled and the cross sections were characterized under SEM (Figure 3A,B). For the CNT−textile anode, a microbial biofilm was wrapped around each CNT−textile fiber, including both exterior and interior fibers (Figure 3A), indicating that the open macroscale porous structure of the CNT−textile can provide sufficient substrate transport inside the CNT−textile anode to maintain internal colonization, consistent with our schematic demonstration in Figure 1A, right. Assuming that all of the CNT−textile fiber surfaces are occupied by biofilms, the anolyte−biofilm−anode interfacial area is calculated to be 10-fold larger than the projective surface of the anode. In the case of the carbon cloth anode, however, microbial colonization was largely restricted to the outer surface of the anode, with few microorganisms present on the interior fibers, as evidenced in Figure 3B. Few microorganisms were observed on the inner surface of the porous carbon cloth anode, suggesting poor substrate transport inside the anode. Improved media flow through the carbon cloth anode may achieve internal microbial colonization, thus improving the MFC performance.[10] However, additional energy would be required to maintain this flow, and clogging would likely be a concern. Therefore, compared with the carbon cloth, our CNT−textile is a true 3D anode with a much higher active surface area for biofilm growth, which should result in improved MFC performance.[38]

Besides the increase in the anolyte−biofilm−anode interfacial area, the CNT−textile fiber surface reveals excellent interaction with the microbial biofilm because all three pathways of electron transfer from exoelectrogens to a CNT−textile anode are likely facilitated by the particular structure and properties of the CNT layer (Figure 1A, right). First, the CNT coating makes the surface of CNT−textile fibers rough (Figure 1C,E). For a single exoelectrogen with a fixed size, the rough surfaces of CNT−textile fibers provide more contact area than

DOI: 10.1021/nl103905t | *Nano Lett.* **XXXX,** *xxx,* 000–000

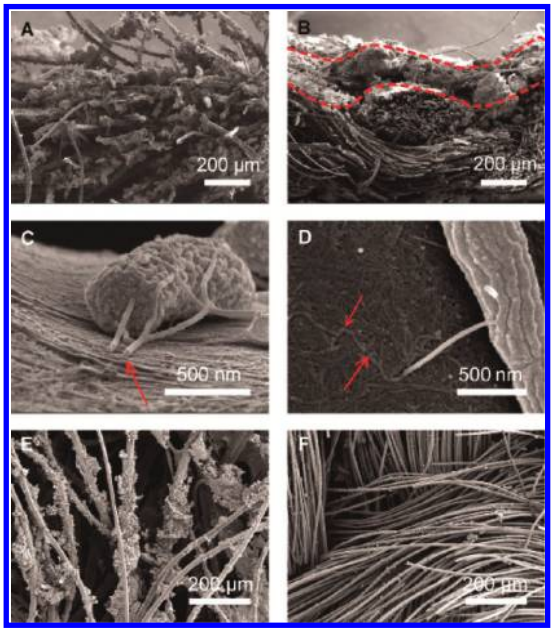

FIGURE 3. SEM images of the microbial growth on the CNT−textile and the carbon cloth. (A) Cross section of the CNT−textile anode illustrating internal colonization. A microbial biofilm wraps around each CNT−textile fiber, including both exterior and interior fibers. (B) Cross section of the carbon cloth anode. The biofilm is largely restricted to the outer surface of the carbon cloth anode (area between two broken lines), with few microorganisms present on the interior fibers. (C) Microbial nanowire extending from the cell membrane and penetrating the CNT layer. (D) Microbial nanowire compactly attaching to the CNT layer. The arrows in C and D indicate the nanowires. (E, F) Projective surface of the CNT−textile anode (E) and the carbon cloth anode (F) after 5 min of bath sonication (100 W) and 10 s of vortex agitation (2700 rpm). Biofilms are still visible on the CNT−textile fibers (E) but not on the carbon cloth fibers (F), suggesting stronger mechanical binding of the microbial biofilm to the CNT−textile anode.

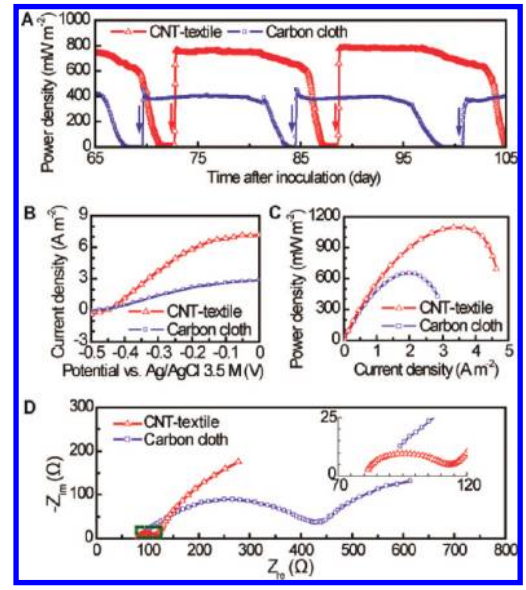

FIGURE 4. Performance of MFCs equipped with different anodes (CNT−textile vs carbon cloth). (A) Repeatable power generation cycles with a 1 kΩ loading. Arrows indicate glucose feeding (0.15 g for 0.15 L of analyte). Power outputs are normalized to the projective surface area of the anode. (B) Linear staircase voltammograms showing that the maximum current density achieved by the CNT−textile anode is 2.6 times that achieved by the carbon cloth anode (7.2 vs 2.8 A m^{-2}). (C) Polarization curve showing that the maximum power density of the MFC prepared with the CNT−textile anode is 68% higher than that prepared with the carbon cloth anode (1098 vs 655 mW m^{-2}). (D) Nyquist curve of the electrochemical impedance spectroscopy test for the microbial fuel cells equipped with the CNT−textile anode and the carbon cloth anode, respectively. The area within the green square is magnified in an inset graph. The charge-transfer resistance between the CNT−textile anode and the electrolyte, indicated by the diameter of the first semicircle of the Nyquist curve, is 10% of the resistance between the carbon cloth anode and the electrolyte (approximately 30 vs 300 Ω).

the smooth surfaces of carbon cloth fibers (Figure 1A), which may resulting in stronger mechanical binding and more efficient electron transfer between cell membranes and the anode. Second, the coated CNTs themselves form a secondary microscale porous structure. This provides high surface area with active functional groups to collect electrons from electron mediators or shuttles in the electrolyte. A recently published study showed that electron transfer by mediators or shuttles was predominant in a model system.[39] Therefore, the increase in active surface area gained from the porous CNT layer benefits the electron transfer significantly. Finally, the CNT layer displays effective interaction with microbial nanowires. A great number of nanowires were observed under SEM (Figure S7). These nanowires (or pili) tethered cells to the anode surface, facilitating the maintenance of a stable biofilm.[40] Nanowires could also be conductive and provide a third route for electron transfer.[41−43] Figure 3C shows a nanowire bridging the gap between CNTs and penetrating the anode surface, and Figure 3D shows a nanowire compactly attached to the CNT layer. These interactions likely enhance the nanowires' functions as tethers and electron conductors, further improving the mechanical binding and electrical conductivity between exoelectrogens and anode materials. This would not be possible for the solid surface of carbon cloth fibers (Figure 1A, left). A simple experiment was performed to assess the strength of the mechanical binding of microbial biofilms to the CNT−textile anode. Anode samples with associated mature microbial biofilms (Figure S8) were sonicated in phosphate buffer solution for 5 min and then subjected to vortex agitation for 10 s. Biofilms remained visible on the CNT−textile fibers (Figure 3E) but not on the carbon cloth (Figure 3F), suggesting stronger mechanical binding of biofilms to the CNT−textile anode than to the carbon cloth anode.

With all of the possible improvements discussed above, the MFC equipped with a CNT−textile anode achieved much better performance than that prepared with a carbon cloth anode. Comparisons were made after 2 months of operation when both of the MFCs achieved repeatable power generation cycles with a 1 kΩ external resistor (Figure 4A). The open circuit potential of both anodes was about −0.45 V versus Ag|AgCl. With the 1 kΩ loading, the potential of the CNT−textile and the carbon cloth dropped to −0.34 and −0.25 V versus Ag|AgCl, respectively. The CNT−textile

DOI: 10.1021/nl103905t | Nano Lett. XXXX, xxx, 000–000

showed a 0.09 V less anodic potential loss than the carbon cloth (0.11 vs 0.20 V). Maximum current density and power density measurements were applied 30 h after the replacement of fresh glucose media, when the power generation returned to steady state and the glucose concentration was still close to the original level (1 g L^{-1}). Both the current density and power density results were normalized to the projective surface area of the anode. As shown in Figure 4B, the maximum current density achieved by the CNT−textile anode was 7.2 A m^{-2}, which is 2.6 times that achieved by the carbon cloth anode under identical conditions (2.8 A m^{-2}). With the same cathode, the maximum power density of the MFC prepared with the CNT−textile anode was 68% higher than that obtained with the carbon cloth anode (1098 vs 655 mW m^{-2}), as determined by the polarization curve (Figure 4*C*). The total electric energy generation of the MFCs can be calculated by integrating the power−time curve (Figure 4A). The results show that the MFC equipped with a CNT−textile anode produced 141% more energy from the same mass of added glucose. These data strongly suggest that a CNT−textile anode enables superior performance.

Electrochemical impedance spectroscopy (EIS) tests were carried out to investigate the internal resistance of both MFCs. The charge-transfer resistance is indicated by the diameter of the first semicycle in the Nyquist curve.[44] As shown in Figure 4D, the charge-transfer resistance of the MFC with the CNT−textile is about 30 Ω whereas that of the MFC with the carbon cloth anode is about 300 Ω. This 10-fold improvement in charge-transfer resistance strongly suggests that the superior performance of the CNT−textile relative to that of conventional carbon cloth anodes is due in large part to the much higher electron-transfer efficiency of this material. The higher electron-transfer efficiency, in turn, likely results from both the increased anolyte−biofilm−anode interfacial surface area and the improved interaction between the anode surface and the microbial biofilm. Future studies are still needed to understand the fractions of the improvement due to these two different mechanisms.

In summary, we have designed and realized highly conductive, 3D, macroscale porous CNT−textile electrodes. This novel anode material affords an open structure for biofilm growth, enabling efficient substrate transport and internal colonization by a diverse microflora. The CNT layer coated onto these electrodes also promotes active surface interaction with the microbial biofilm and facilitates electron transfer from exoelectrogens to CNT−textile anodes, thus resulting in high-power operation of MFCs. Our work provides a new platform for designing high-performance MFC anodes that is promising for large-scale practical application.

Acknowledgment. We thank Dr. Lydia-Marie Joubert and Brad Eggleston for experimental assistance. This work was made possible by the King Abdullah University of Science and Technology (KAUST) Investigator Award (no. KUS-l1-001-12). X.X. acknowledge support from the Stanford Graduate Fellowship.

Supporting Information Available. Supplementary Figures S1−S8 and a detailed Materials and Methods section, including CNT−textile synthesis, MFC construction and operation, and electrochemical and biological characterization. This material is available free of charge via the Internet at http://pubs.acs.org.

REFERENCES AND NOTES

(1) Logan, B. E. *Nat. Rev. Microbiol.* **2009**, *7*, 375.
(2) Rittmann, B. E.; Krajmalnik-Brown, R.; Halden, R. U. *Nat. Rev. Microbiol.* **2008**, *6*, 604.
(3) Lovley, D. R. *Nat. Rev. Microbiol.* **2006**, *4*, 497.
(4) Rabaey, K.; Verstraete, W. *Trends Biotechnol.* **2005**, *23*, 291.
(5) Chaudhuri, S. K.; Lovley, D. R. *Nat. Biotechnol.* **2003**, *21*, 1229.
(6) Liu, H.; Ramnarayanan, R.; Logan, B. E. *Environ. Sci. Technol.* **2004**, *38*, 2281.
(7) Tender, L. M.; Reimers, C. E.; Stecher, H. A.; Holmes, D. E.; Bond, D. R.; Lowy, D. A.; Pilobello, K.; Fertig, S. J.; Lovley, D. R. *Nat. Biotechnol.* **2002**, *20*, 821.
(8) Konikoff, J. J.; Reynolds, L. W.; Harris, E. S. *Aerosp. Med.* **1963**, *34*, 1129.
(9) Torres, C. I.; Marcus, A. K.; Lee, H. S.; Parameswaran, P.; Krajmalnik-Brown, R.; Rittmann, B. E. *FEMS Microbiol. Rev.* **2010**, *34*, 3.
(10) Cheng, S.; Liu, H.; Logan, B. E. *Environ. Sci. Technol.* **2006**, *40*, 2426.
(11) Min, B.; Logan, B. E. *Environ. Sci. Technol.* **2004**, *38*, 5809.
(12) He, Z.; Minteer, S. D.; Angenent, L. T. *Environ. Sci. Technol.* **2005**, *39*, 5262.
(13) Logan, B. E.; Cheng, S.; Watson, V.; Estadt, G. *Environ. Sci. Technol.* **2007**, *41*, 3341.
(14) Scott, K.; Rimbu, G. A.; Katuri, K. P.; Prasad, K. K.; Head, M. I. *Process Saf. Environ. Prot.* **2007**, *85*, 481.
(15) Jiang, D. Q.; Li, B. K. *Water Sci. Technol.* **2009**, *59*, 557.
(16) Tsai, H. Y.; Wu, C. C.; Lee, C. Y.; Shih, E. P. *J. Power Sources* **2009**, *194*, 199.
(17) Qiao, Y.; Bao, S. J.; Li, C. M.; Cui, X. Q.; Lu, Z. S.; Guo, J. *ACS Nano* **2008**, *2*, 113.
(18) Zou, Y. J.; Xiang, C. L.; Yang, L. N.; Sun, L. X.; Xu, F.; Cao, Z. *Int. J. Hydrogen Energy* **2008**, *33*, 4856.
(19) Qiao, Y.; Li, C. M.; Bao, S. J.; Bao, Q. L. *J. Power Sources* **2007**, *170*, 79.
(20) Pham, T. H.; Aelterman, P.; Verstraete, W. *Trends Biotechnol.* **2009**, *27*, 168.
(21) Schroder, U. *Phys. Chem. Chem. Phys.* **2007**, *9*, 2619.
(22) Kim, B. H.; Chang, I. S.; Gadd, G. M. *Appl. Microbiol. Biotechnol.* **2007**, *76*, 485.
(23) Hu, L.; Pasta, M.; Mantia, F. L.; Cui, L.; Jeong, S.; Deshazer, H. D.; Choi, J. W.; Han, S. M.; Cui, Y. *Nano Lett.* **2010**, *10*, 708.
(24) Gao, F.; Viry, L.; Maugey, M.; Poulin, P.; Mano, N. *Nat. Commun.* **2010**, *1*, 2.
(25) Lim, J.; Malati, P.; Bonet, F.; Dunn, B. *J. Electrochem. Soc.* **2007**, *154*, A140.
(26) Wang, C.; Waje, M.; Wang, X.; Tang, J. M.; Haddon, R. C.; Yan, Y. S. *Nano Lett.* **2004**, *4*, 345.
(27) Kang, S.; Pinault, M.; Pfefferle, L. D.; Elimelech, M. *Langmuir* **2007**, *23*, 8670.
(28) Magrez, A.; Kasas, S.; Salicio, V.; Pasquier, N.; Seo, J. W.; Celio, M.; Catsicas, S.; Schwaller, B.; Forro, L. *Nano Lett.* **2006**, *6*, 1121.
(29) Hashsham, S. A.; Fernandez, A. S.; Dollhopf, S. L.; Dazzo, F. B.; Hickey, R. F.; Tiedje, J. M.; Criddle, C. S. *Appl. Environ. Microbiol.* **2000**, *66*, 4050.
(30) Fernandez, A. S.; Hashsham, S. A.; Dollhopf, S. L.; Raskin, L.; Glagoleva, O.; Dazzo, F. B.; Hickey, R. F.; Criddle, C. S.; Tiedje, J. M. *Appl. Environ. Microbiol.* **2000**, *66*, 4058.
(31) Rabaey, K.; Lissens, G.; Siciliano, S. D.; Verstraete, W. *Biotechnol. Lett.* **2003**, *25*, 1531.

DOI: 10.1021/nl103905t | *Nano Lett.* **XXXX,** *xxx,* 000–000

(32) Lee, H. S.; Parameswaran, P.; Kato-Marcus, A.; Torres, C. I.; Rittmann, B. E. *Water Res.* **2008**, *42*, 1501.
(33) Fan, Y. Z.; Hu, H. Q.; Liu, H. *Environ. Sci. Technol.* **2007**, *41*, 8154.
(34) Ahn, Y.; Logan, B. E. *Bioresour. Technol.* **2010**, *101*, 469.
(35) Logan, B. E.; Hamelers, B.; Rozendal, R. A.; Schrorder, U.; Keller, J.; Freguia, S.; Aelterman, P.; Verstraete, W.; Rabaey, K. *Environ. Sci. Technol.* **2006**, *40*, 5181.
(36) Watanabe, K. *J. Biosci. Bioeng.* **2008**, *106*, 528.
(37) Zhao, F.; Slade, R. C. T.; Varcoe, R. *Chem. Soc. Rev.* **2009**, *38*, 1926.
(38) Torres, C. I.; Marcus, A. K.; Rittmann, B. E. *Biotechnol. Bioeng.* **2008**, *100*, 872.
(39) Jiang, X. C.; Hu, J. S.; Fitzgerald, L. A.; Biffinger, J. C.; Xie, P.; Ringeisen, B. R.; Lieber, C. M. *Proc. Natl. Acad. Sci. U.S.A.* **2010**, *107*, 16806.
(40) Reguera, G.; Pollina, R. B.; Nicoll, J. S.; Lovley, D. R. *J. Bacteriol.* **2007**, *189*, 2125.
(41) Reguera, G.; McCarthy, K. D.; Mehta, T.; Nicoll, J. S.; Tuominen, M. T.; Lovley, D. R. *Nature* **2005**, *435*, 1098.
(42) Gorby, Y. A.; Yanina, S.; McLean, J. S.; Rosso, K. M.; Moyles, D.; Dohnalkova, A.; Beveridge, T. J.; Chang, I. S.; Kim, B. H.; Kim, K. S.; Culley, D. E.; Reed, S. B.; Romine, M. F.; Saffarini, D. A.; Hill, E. A.; Shi, L.; Elias, D. A.; Kennedy, D. W.; Pinchuk, G.; Watanabe, K.; Ishii, S.; Logan, B.; Nealson, K. H.; Fredrickson, J. K. *Proc. Natl. Acad. Sci. U.S.A.* **2006**, *103*, 11358.
(43) El-Naggar, M. Y.; Wanger, G.; Leung, K. M.; Yuzvinsky, T. D.; Southam, G.; Yang, J.; Lau, W. M.; Nealson, K. H.; Gorby, Y. A. *Proc. Natl. Acad. Sci. U.S.A.* **2010**, *107*, 18127.
(44) He, Z.; Mansfeld, F. *Energy Environ. Sci.* **2009**, *2*, 215.

DOI: 10.1021/nl103905t | *Nano Lett.* **XXXX,** *xxx,* 000–000